Cartographer in the Loop: Interactive Land Cover Change Detection Using Geospatial Foundation Model Embeddings

Xihan Yao[1,*], **Koutian Wu**[2], **Rushi Bhatt**[1], **Brendon Hall**[3], and **Yuhao Kang**[1]

[1] *Department of Geography and the Environment, University of Texas at Austin, Austin, TX, USA*

[2] *Jackson School of Geosciences, University of Texas at Austin, Austin, TX, USA*

[3] *Deloitte, Houston, TX, USA*

* *xyaoaf@utexas.edu*

Keywords: change detection, geospatial foundation models, remote sensing, land cover, interactive cartography, human-in-the-loop

Introduction

Land cover change is among the most consequential processes shaping our natural and built environments. Detecting where, when, and how substantially the land surface has changed — from wildfire scars and urban expansion to deforestation, agricultural intensification, and irrigation development — is fundamental to environmental monitoring, disaster response, urban planning, and climate research. Advances in satellite remote sensing have made annual global coverage routine, yet transforming petabytes of orbital observations into interpretable change maps still demands human expertise to contextualize, verify, and communicate findings. This tension between algorithmic automation and expert human judgment is precisely what the CaGIS 2026 theme, *The Cartographer in the Loop*, addresses.

This extended abstract presents ongoing research — originating as a winning project at the UT Austin Geoscience Hackathon — on an interactive land cover change detection system grounded in geospatial foundation model embeddings. The system is designed to augment rather than replace the cartographer's interpretive role. The central research question is: *Can learned representations from a geospatial foundation model provide a reliable and generalizable signal for spatiotemporal land cover change detection across diverse land cover types, and how does an interactive human-in-the-loop interface enhance the analyst's ability to explore, verify, and interpret such detections?*

Our approach uses AlphaEarth (Brown et al., 2025), a geospatial foundation model that compresses multi-source annual satellite observations into 64-dimensional learned embeddings at 10-meter resolution globally from 2017 to 2024. By computing cosine dissimilarity between consecutive yearly embedding vectors, we detect semantic changes in land surface character without spectral index selection or land-cover-specific parameter tuning. We compare against LandTrendr (Kennedy et al., 2018), a well-validated NDVI-based spectral trajectory method, across 15 study sites spanning urbanization, wildfire, and forest harvesting.

Method

AlphaEarth Change Detection Pipeline

For a user-defined area of interest (AOI), annual AlphaEarth embeddings are loaded from the Google Earth Engine (GEE) collection GOOGLE/SATELLITE_EMBEDDING/V1/ANNUAL (Gorelick et al., 2017) for 2017–2024. Each pixel is represented by a 64-dimensional vector v encoding optical, radar, elevation, and climate inputs. Vectors are L2-normalized to the unit hypersphere, so that the dot product equals the cosine similarity:

$$sim(v_t, v_{t+1}) = v_t \cdot v_{t+1}$$

Dissimilarity between consecutive years is then:

$$d(t, t+1) = 1 - sim(v_t, v_{t+1})$$

We compute *d* for all seven consecutive year-pairs (2017→2018 through 2023→2024). The three standardized change layers are derived as:

$$YOD = arg\ max_t\ \ d(t, t+1)$$
$$MAG = max_t\ \ d(t, t+1)$$
$$DUR = |\{t : d(t, t+1) > \tau\}|$$

where YOD is the year of detected change, MAG is the maximum dissimilarity, DUR is the count of high-change year-pairs, and τ is a user-adjustable magnitude threshold (default $\tau = 0.15$). A Gaussian spatial smoothing kernel (radius = 2 pixels, $\sigma = 1$) is applied to MAG before thresholding, reducing salt-and-pepper noise. All computation runs server-side in GEE via the *compute_alpha_layers()* and *smooth_and_mask_alpha()* modules.

LandTrendr Comparison

Fifteen pre-computed LandTrendr GEE assets derived from Landsat NDVI time series (2016–2024) serve as the baseline. Both methods produce identical standardized outputs (YOD, MAG, DUR), enabling direct comparison. A magnitude threshold of |MAG| > 170 NDVI units and equivalent Gaussian smoothing produce binary LandTrendr change masks. Intersection over Union (IoU) between the two methods' binary masks is computed per site in a single batched GEE request.

Study Sites

The 15 sites cover three categories of land cover change across the western United States: urbanization (Austin TX, Dallas TX, Houston TX, Portland OR, Bend OR, Sacramento CA), wildfire (Camp Fire CA 2018, Santiam OR 2020, Bootleg OR 2021, Dixie CA 2021, Mosquito CA 2022), and forest harvesting (Angelina TX, Coos Bay OR, Mt Hood OR, Shasta-Trinity CA). Sites were selected to span a range of change magnitudes, durations, and ecological contexts, enabling broad evaluation of the AlphaEarth signal.

Interactive Inspection Interface

The detection pipeline is paired with a Jupyter-based interactive tool built with geemap and ipyleaflet. Users draw a polygon or rectangle AOI on a web map and trigger server-side GEE computation of all change layers (~30 seconds). Results appear as toggleable map layers: raw and smoothed MAG, YOD color-coded by year, DUR, and binary change mask. A point inspector allows users to click any location inside the AOI and receive a popup chart showing year-by-year cosine dissimilarity — the raw temporal signal underlying the automated detection (Figure 2). Parameter sliders (magnitude threshold, smoothing radius/sigma, layer opacity) allow real-time sensitivity exploration. Layers can be exported to GEE Assets or Google Drive.

Results

The IoU analysis across 15 sites reveals systematic variation by change type (Figure 1). Wildfire sites show the highest agreement between AlphaEarth and LandTrendr (IoU: 0.61–0.79), consistent with large abrupt NDVI drops captured by both methods. Urban sites show lower agreement (IoU: 0.29–0.53), suggesting AlphaEarth captures surface change signals — potentially from radar and structure-sensitive inputs — that NDVI-based LandTrendr does not. Forest harvesting sites show intermediate agreement (IoU: 0.60–0.76) with site-level variability.

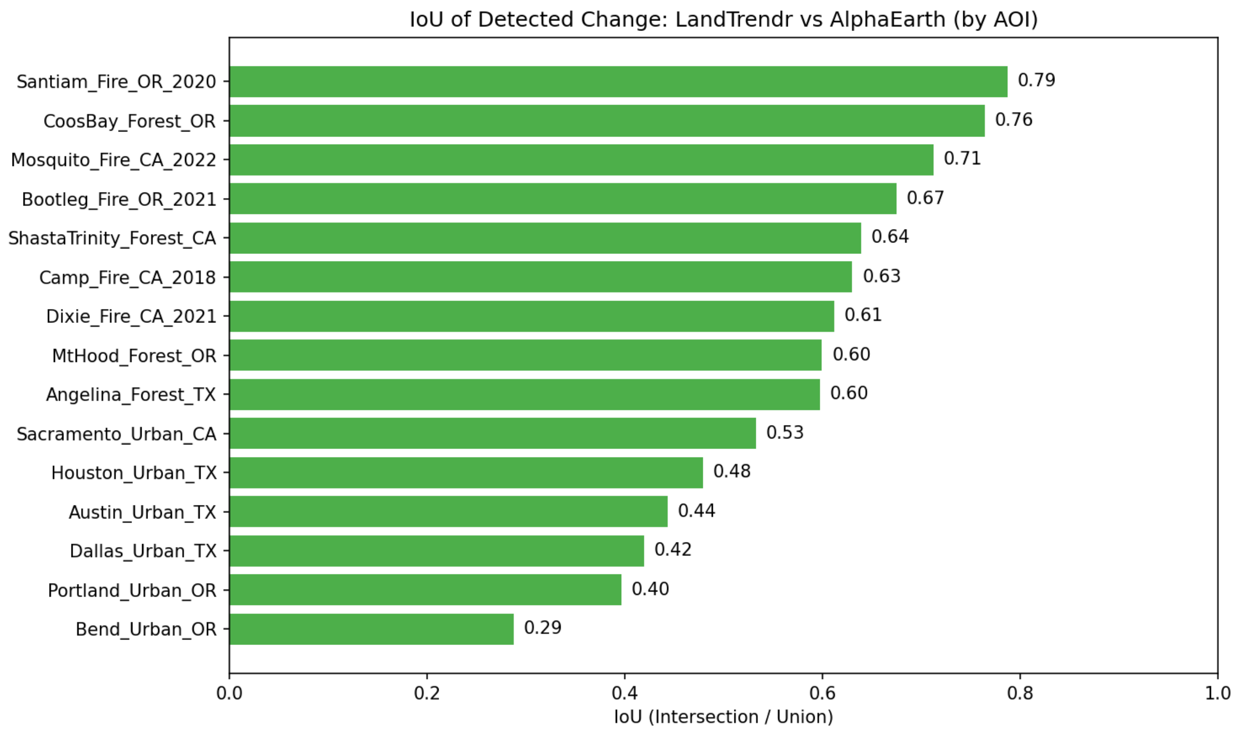

Figure 1. IoU scores comparing AlphaEarth and LandTrendr binary change masks across all 15 study sites, sorted by score. Higher IoU indicates stronger spatial agreement between the two methods.

The Austin, TX site (Figure 3) illustrates the urban change signal: high-magnitude detections cluster on the city's rapidly expanding periphery, co-locating with known construction corridors and new developments. The change magnitude map produced by AlphaEarth captures these impervious surface transitions that LandTrendr often misses due to its NDVI foundation.

Qualitative case studies highlight cross-domain applicability beyond the 15-site benchmark. The destruction of the Nova Kakhovka Dam in Ukraine (June 2023) is detected with high confidence, with YOD consistent with the known event date. Pivot irrigation expansion in Eritrea produces strong cosine dissimilarity signatures visible at the country scale, demonstrating agricultural monitoring capability without any modification or retraining.

The point inspector reveals interpretable temporal signal shapes that go beyond what a binary change map conveys: wildfire sites show a sharp dissimilarity spike in the event year followed by gradual decline as vegetation recovers; urban sites show sustained elevated dissimilarity over multiple consecutive years consistent with multi-phase construction; irrigation sites show a step-change signal at the onset of agricultural infrastructure. This temporal signature differentiation is directly accessible to the analyst through the inspector tool (Figure 2).

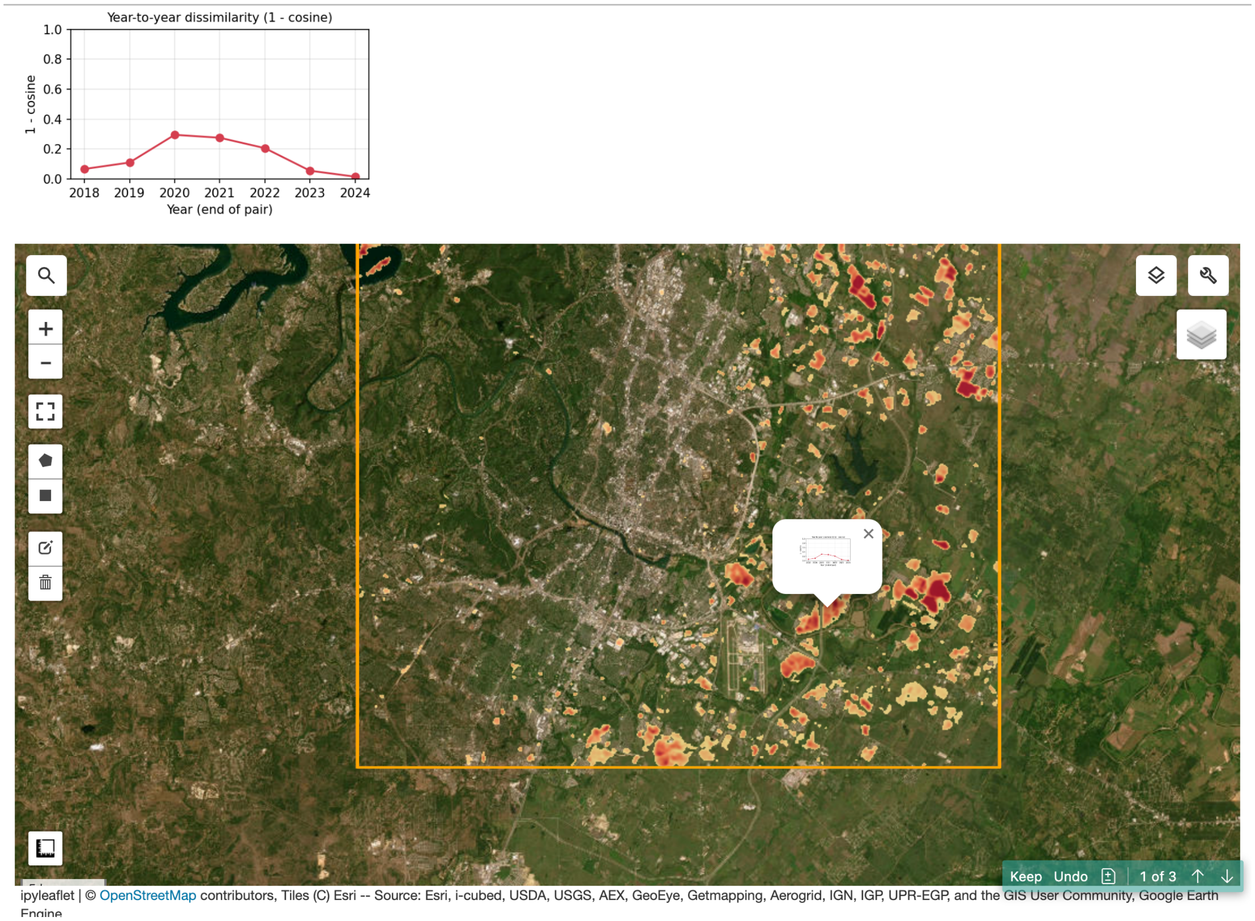

Figure 2. Interactive point inspector showing year-to-year cosine dissimilarity at a selected location in Austin, TX. The popup chart (upper left) allows analysts to examine the temporal signal underlying any detected change, supporting qualitative interpretation of change type.

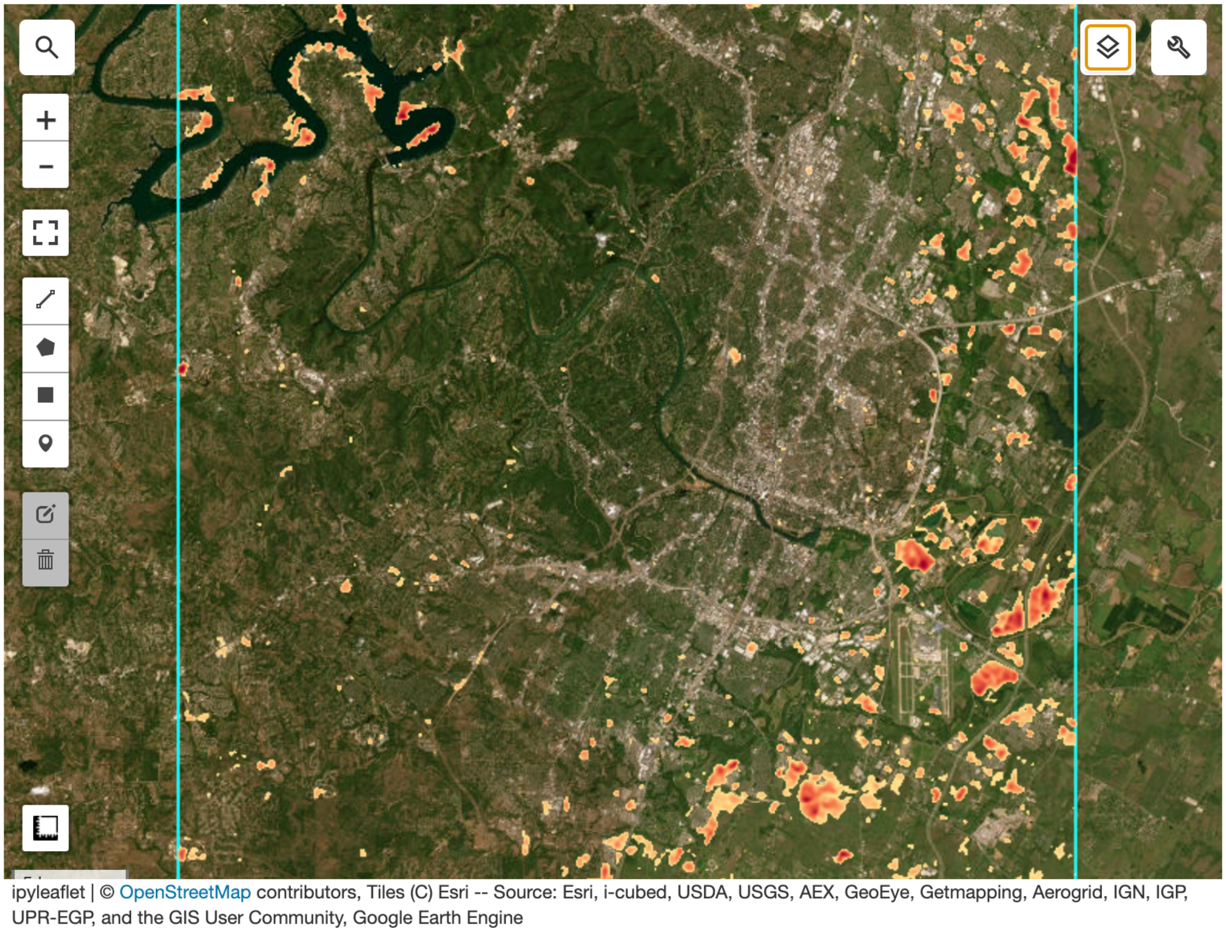

Figure 3. AlphaEarth change magnitude map for the Austin, TX study area (2017–2024). Detected changes (orange–red) are overlaid on Esri WorldImagery, highlighting urban expansion on the city periphery.

Discussion and Conclusion

This work contributes at two levels. Methodologically, we demonstrate that cosine dissimilarity in learned embedding space from a geospatial foundation model constitutes a viable change detection signal across structurally diverse land cover change types — wildfire, urban growth, forest harvesting, and irrigated agriculture — without per-type spectral index selection or parameter calibration. This unified metric opens the possibility of globally consistent, multi-type change mapping within a single workflow.

At the tool level, the interactive inspection interface instantiates the 'cartographer in the loop' design principle concretely. Automated detection provides the geographic hypothesis: a map of where and when change likely occurred. The human analyst uses the temporal inspector to examine the underlying evidence at specific locations, adjust detection sensitivity, and form interpretive understanding of what changed and why. The cartographer is positioned as an active interpretive partner rather than a passive consumer of algorithmic output.

Broader significance lies in accessibility. By grounding detection in a foundation model embedding rather than a domain-specific index, the method reduces the prerequisite knowledge needed to apply change detection across unfamiliar landscapes. A cartographer who understands geography but not remote sensing spectroscopy can meaningfully engage with detection results, form spatial hypotheses, and validate them through point inspection — consistent with the conference's inquiry into how GeoAI can expand practitioner expertise while respecting the irreplaceable value of human judgment.

This work is ongoing. Future work will validate against authoritative reference datasets — MTBS fire perimeters for wildfire sites, NLCD land cover transitions for urban sites, and FAO cropland layers for agricultural sites — to quantify Precision, Recall, and F1 per change category. A fully web-deployable interface is planned to extend access beyond the research community.

Acknowledgements

This project originated at the UT Austin Geoscience Hackathon, where Team Alpha received first place. The authors thank the hackathon organizers and the Google Earth Engine team for data access. AlphaEarth embeddings are provided through the GOOGLE/SATELLITE_EMBEDDING/V1/ANNUAL GEE collection.

References

Brown, C. F., et al. (2025). AlphaEarth Foundations. *arXiv:2507.22291*.

Gorelick, N., Hancher, M., Dixon, M., Ilyushchenko, S., Thau, D., & Moore, R. (2017). Google Earth Engine: Planetary-scale geospatial analysis for everyone. *Remote Sensing of Environment*, 202, 18–27. doi: 10.1016/j.rse.2017.06.031

Janowicz, K., Gao, S., McKenzie, G., Hu, Y., & Bhaduri, B. (2020). GeoAI: Spatially explicit artificial intelligence techniques for geographic knowledge discovery and beyond. *International Journal of Geographical Information Science*, 34(4), 625–636. doi: 10.1080/13658816.2019.1684500

Kennedy, R. E., Yang, Z., & Cohen, W. B. (2010). Detecting trends in forest disturbance and recovery using yearly Landsat time series: 1. LandTrendr — temporal segmentation algorithms. *Remote Sensing of Environment*, 114(12), 2897–2910. doi: 10.1016/j.rse.2010.07.008

Kennedy, R. E., Yang, Z., Gorelick, N., Braaten, J., Cavalcante, L., Cohen, W. B., & Healey, S. (2018). Implementation of the LandTrendr algorithm on Google Earth Engine. *Remote Sensing*, 10(5), 691. doi: 10.3390/rs10050691

MacEachren, A. M. (1995). *How Maps Work: Representation, Visualization, and Design*. New York, NY: Guilford Press.

Roth, R. E. (2013). Interactive maps: What we know and what we need to know. *Journal of Spatial Information Science*, 6, 59–115. doi: 10.5311/JOSIS.2013.6.105